## Research Article

# Cyclophilin 40 alters UVA-induced apoptosis and mitochondrial ROS generation in keratinocytes

*Jana Jandova*[*,1], *Jaroslav Janda*[1], *James E. Sligh*

Southern Arizona VA Healthcare System and the Department of Medicine, Division of Dermatology and Arizona Cancer Center, University of Arizona, 1515N Campbell Avenue, Tucson, AZ, USA

### ARTICLE INFORMATION

### ABSTRACT

The CyP40 protein encoded by PPID gene is a member of the peptidyl-prolyl cis–trans isomerase (PPIase) family. PPIases catalyze the cis–trans isomerization of proline imidic peptide bonds in oligopeptides and accelerate the folding of proteins. The CyP40 protein has been shown to possess PPIase activity and, similar to other family members, can bind to the immunosuppressant drug cyclosporin A (CsA). In this study, we created keratinocyte cell lines with CyP40 being stably knocked down using viral particles containing shRNA for CyP40 which knocked down the expression level of CyP40 transcripts by 90–99%. The proliferation rates of the cell lines with silenced CyP40 were decreased compared to the control cells. After UVA irradiation, the rate of apoptosis was found to be significantly lower in CyP40 silenced cell lines than it was in control cells. Moreover, mitochondrial membrane potential (MMP) was found to be less dissipated and mitochondrial permeability transition pore (MPTP) less active in cells with knocked down CyP40 than in control cells after UVA irradiation. Also, less mitochondrial superoxide was detected in the cells with silenced CyP40 compared to control cells after UVA exposure. Moreover, silencing of CyP40 partially modulates expression of key genes involved in mitochondrial pore formation including CyPD, ANTs and VDAC family members. The ability of CyP40 to regulate UV induced apoptosis implicates this protein as a potential target for therapy in cancer cells.

## Introduction

Cyclophilin proteins (CyPs) are ubiquitous proteins with peptidyl-prolyl cis–trans isomerase activity [1]. CyPs are highly conserved among all types of species including animals, plants, fungi and bacteria with a shared isomerase domain of approximately 109 amino acids. In humans, there are sixteen CyPs including cyclophilin 40, a 40 kD cytosolic protein (CyP40)

---

encoded by the PPID gene which is also referred to in some literature as cyclophilin D (CyPD). There exists some confusion in the nomenclature whereby an additional CyP member is also referred to as cyclophilin D, which is the 17 kD mitochondrial protein involved in MPTP regulation.

The 17 kDa mitochondrial cyclophilin D (CyPD) encoded by PPIF gene regulates MPTP function and plays a crucial role in cell death [2]. The MPTP is a high conductance channel of the inner mitochondrial membrane whose opening allows flux of molecules of ≤1.5 kDa [3]. The other regulatory and structural components of the MPTP are thought to include voltage-dependent-anion-channel (VDAC) family members, non-specific pore proteins located in the outer mitochondrial membrane and the adenine-nucleotide-translocators (ANTs), specific ATP/ADP transporters, located in the inner mitochondrial membrane. CyPD is known to be associated with ANT in the matrix of mitochondria. The MPTP starts its formation in response to conditions of cellular stress including mitochondrial calcium overload, oxidative stress, elevated phosphate concentration and adenine depletion and the consequence of this process for the cell is MPTP fluxing [4,5]. The opening of the mitochondrial permeability transition pore causes a collapse of the mitochondrial membrane potential, leading to ATP depletion and cell death, depending on the rate of ATP consumption. MPTP opening can trigger different types of cell death. Transient opening results in the release of cytochrome c, which activates the caspase cascade and triggers apoptosis. Sustained pore opening results in the uncoupling of oxidative phosphorylation what limits ATP synthesis and leads to necrotic cell death.

CyP40, the product of PPID gene, is a cytosolic protein containing 370 amino acids and shares many structural features of the mitochondrial CyPD [6]. CyP40 functions include contributing to protein folding, ligand binding, and nuclear localization of glucocorticoid, estrogen and progesterone receptors [7–9]. In terms of protein folding, one of the most important roles of CyP40 is to help with assembling of heat shock protein Hsp90 in chaperone protein-folding machinery [10]. CyP40 shares structural and sequence homology with FKBP51 and FKBP52, proteins of the FK506-binding class identified as common components of steroid receptor complexes. These three large immunophilins (CyP40, FKBP51, FKBP52) are characterized by an N-terminal immunophilin-like domain together with a conserved C-terminal tetratricopeptide repeat (TPR) domain that provides an interface for protein interaction [11]. All target an identical site within Hsp90 through this conserved C-terminal region to form separate steroid receptor complexes containing Hsp90 associated with a single cytosolic immunophilin [12].

The role of 40 kDa CyP40 in cancer pathogenesis has not been extensively investigated, although some recent reports showed certain expression correlations of this cyclophilin in cancer cells. Periyasamy et al. [13] have previously showed that levels of FKBP52, FKBP51 and CyP40 are high in prostate cancer cells lines (LNCaP, PC-3, and DU145) compared to primary prostate cells and provided the first evidence that CsA and FK506 can negatively modulate proliferation of prostate cells in vitro. Ward et al. [14] reported that Cyp40 mRNA was over-expressed in breast cancer tissues as compared with matched normal breast control tissues, and Cyp40 mRNA was ubiquitously expressed in 10 breast cancer cell lines. The breast cancer cell line MCF-7 showed a 75-fold increase of Cyp40 mRNA expression in response to high temperature stress and marked redistribution of Cyp40 protein

from a predominantly nuclear location to nuclear accumulation [15]. In addition to Cyp40 up-regulation, Ward et al. [16] also reported that genetic analysis of breast cancer patients heterozygous for Cyp40 showed 30% Cyp40 allelic loss. This indicates that dysregulation of CyP40 either as up-regulation of CyP40 gene expression or as loss of function could have pro-tumorigenic effects.

One of the most studied phenomena related to cyclophilins is their interaction with immunosuppressant drugs. The ability of CyP40 to bind the immunosuppressive drugs FK506 and CsA has served to categorize this protein as immunophilin. Binding of CsA to immunophilins causes inhibition of the protein's PPIase activity. The inhibition of PPIase activity is thought to ultimately contribute to the protection of cells from undergoing apoptosis [17]. CsA interacts with many cyclophilin proteins including 17 kDa CyPD located in the mitochondrial matrix leading to inhibition of MPTP formation [18] and inhibition of cell death pathways mediated by this pore [19]. This interaction was shown to be an effective therapeutic tool in limiting acute myocardial infarction and in correcting mitochondrial dysfunction in myopathies [20]. CsA also interacts with cytoplasmic 40 kDa CyPD (CyP40), although its affinity for this receptor is lower than the mitochondrial 17 kDa CyPD. The weak affinity of CyP40 for CsA was postulated to arise from a histidine (His) residue that replaces a tryptophan (Trp) residue critical for CsA binding which is highly conserved in other cyclophilins that have high affinity for CsA. Site-directed mutagenesis to replace His141 by Trp yielded a protein with an approximately 20-fold greater affinity for cyclosporin A. Thus replacing the His141 (in CyP40) by Trp (in CyPD) is likely to be critical for determining binding affinity to CsA [21].

Apoptosis is a complex pathway involving several stages starting from pre-apoptotic signals through mitochondrial collapsing to the ultimate cell death. Apoptosis can be induced by various factors of biological, chemical and physical origin. One of the well known physical agents triggering apoptotic processes in cells is UV light which directly damages DNA and leads to high ROS production [22].

The intrinsic apoptotic pathway is mediated through mitochondria and thus 17 kDa mitochondrial CyPD is directly involved in this process. There is a support for mitochondrial CyPD role in UVA-induced apoptosis and cell death processes [23,24] as well as a large amount of evidence that UVA light is responsible for cellular apoptosis mediated through the stimulation of ROS production [25,26]. However, there are only very limited data available on the role of cytosolic CyP40 in apoptosis generally and no reports about its role in UVA-induced apoptosis specifically. The aim of this research is to elucidate the effect of cytosolic CyP40 on UVA-induced apoptosis and related mitochondrial processes including ROS production in keratinocytes with altered expression of Cyp40 gene.

## Materials & methods

### Cells and media

HaCaT cells of keratinocyte origin were cultured in DMEM medium (Invitrogen, San Diego, CA) supplemented with 10% FBS (Hyclone, Logan, UT) and penicillin/streptomycin (50 μg/ml) (Invitrogen, San Diego, CA). Transfected HaCaT cells were incubated in DMEM media supplemented with 0.5 ug/ml puromycin

(Sigma-Aldrich, Saint Louis, MO). All cells were maintained in a humidified incubator with 5% $CO_2$ at 37 °C.

## Stable shRNA transfection of HaCaT cells

HaCaT cells were transfected with CyP40 shRNA lentiviral transduction particles according to the manufacturer's instructions (Sigma-Aldrich, Saint Louis, MO). Two independent shRNA sequences in pLKO.1 expression vector were used to transfect the cells resulting in creation of two cell lines called PPID-6 and PPID-7. PPID-6 cell line was created from construct TRCN0000049266 (CCGGGTTGGTCGAATTGTCTTAGAACTCGAG-TTCTAAGACAATTCGACCAACTTTTTG) and PPID-7 cell line from construct TRCN0000049267 (CCGGCCTGAGGATGCGGATATA-GATCTCGAGATCTATATCCGCATCCTCAGGTTTTTG). As a control, an empty pLKO.1 vector was used to transfect the HaCaT cells. All resulting PPID-6, PPID-7 and control cells were selected from a single cell colony for each particular construct and puromycin was used as a selective agent since the pLKO.1 vector contains the region for resistance to puromycin.

## RNA extraction

Total RNA was isolated using Qiagen RNeasy Mini Kit (Qiagen Sciences, Gaithersburg, MD) according to the manufacturer's protocol. The RNA integrity was checked by the RNA 6000 Nano chip kit using Agilent 2100 Bioanalyzer (Agilent Technologies, Santa Clara, CA).

## Quantitative real-time reverse transcriptase polymerase chain reaction (RT-PCR)

Human PPID/CyP40 (Hs00234593_m1), β-actin (Hs99999903_m1), PPIF/CyPD (Hs00194847_m1), ANT2 (Hs00854499_g1), ANT3 (Hs00745067_s1) and VDAC1 (Hs01019082_mH) primer/probes were purchased from ABI (Applied Biosystems, Branchburg, NJ). cDNAs were synthesized from 500 ng of total RNA in a 50 ul reaction with master mix containing $10 \times$ RT buffer, 5.5 mM $MgCl_2$, 2 mM dNTPs, 2.5 μM random hexamers, 2 units of RNase inhibitor and 62.5 units of Multi Scribe reverse transcriptase. All master mix reagents were purchased from ABI (Applied Biosystems, Branchburg, NJ). cDNA synthesis was performed in MJ Thermocycler PTC-200 (MJ Research, Inc., Watertown, MA) using these conditions: 25 °C for 10 min, 48 °C for 30 min and 95 °C for 5 min. 10 ng of cDNA was used for RT-PCR under these conditions: 10 min at 95 °C followed by 40 cycles of 15 s at 95 °C, and 1 min at 60 °C using ABI7000 Real-Time PCR System (Applied Biosystems, Foster City, CA). PCR amplification of the human β-actin was used as a control quality for cDNA amplification. Non-template controls were included in each PCR plate. PPID, PPIF, VDAC1, ANT2, ANT3 levels were normalized to β-actin control. Amplification plots were generated and the $C_t$ values (cycle number at which fluorescence reaches threshold) recorded.

## Proliferation assay

Individual cell lines were plated in the 6-well plates at the concentration of $1 \times 10^5$ cells per well. The cells were grown for 24 h, 48 h and 72 h. After each time period the cells were collected and viable cells were counted with a hemocytometer every other day by the trypan blue exclusion method.

## UVA-irradiation

Cells were grown in 6-well plates with removable lids and exposed to either single or serial doses of UVA irradiation. We used the UVA panel (Ultra-lite, Inc.) filled with six lamps (F72T12-BL-HO UVA) that deliver broad band UVA from 320 to 400 nm. The dose of UVA radiation was monitored with UVA meter (National Biological Corporation, Beachwood, OH). 20 $J/cm^2$ dose of the UVA was chosen for all experiments. Non-irradiated cells were incubated at room temperature inside of the cell culture hood at the same time that the other cells were being exposed to UVA.

## Annexin V-FITC apoptosis detection assay

Annexin V-FITC apoptosis detection assay kit from the Biovision (Mountain View, CA) was used to assess the apoptosis of transfected cell lines. Control cells were seeded at a concentration of $1 \times 10^5$ cells per well while the PPID-6 and PPID-7 cells at a concentration of $1.7 \times 10^5$ cells per well in 6-well plates. After 24 h of initial incubation the cultured media were replaced with fresh growing media and the cells were incubated for additional 24 h to obtain the same 50–60% confluence. Then cells were exposed to two irradiations of 20 $J/cm^2$ UVA spaced 12 h apart for a total dose of 40 $J/cm^2$. 4 h after the second irradiation the growing media were collected and remaining cells were trypsinized. Tubes containing collected media and trypsinized cells were centrifuged together and the pellet was resuspended in 0.5 ml of DPBS and Annexin V and PI were added to each tube and tubes were incubated in the dark for 5 min. Apoptosis was detected using flow cytometry (excitation/emission fluorescence is 488/530 nm). Cells negative for both markers were considered viable.

## Flow cytometry

A total of 10,000 events were counted for each sample using a FACScan flow cytometer Canto II (Becton–Dickinson, Franklin Lakes, NJ) equipped with a 488 nm argon laser with appropriate filters. Data were collected from gated cells of appropriate size. Data were analyzed using DIVA software (Becton–Dickinson, Franklin Lakes, NJ).

## Mitochondrial membrane potential assay (JC-1 assay)

JC-1 membrane potential kit from Invitrogen (San Diego, CA) was used according to manufacturer's instructions. Control cells were seeded at a concentration of $1 \times 10^5$ cells per well while the PPID-6 and PPID-7 cells at a concentration of $1.7 \times 10^5$ cells per well in 6-well plates. After 24 h of initial incubation the cultured media were replaced and the cells were incubated for additional 24 h to obtain the same 50–60% confluence. Then cells were exposed to two irradiations of 20 $J/cm^2$ UVA spaced 12 h apart for a total dose of 40 $J/cm^2$. 4 h after the second irradiation the growing media were collected and remaining cells were trypsinized. Tubes containing collected media and trypsinized cells were centrifuged together and the pellet was resuspended in 1 ml of DPBS and loaded with JC-1 fluorescent dye at a final concentration of 2 μM and incubated at 37 °C, 5% $CO_2$ for 30 min. As a control, non-irradiated cells were loaded with JC-1 or simultaneously loaded with JC-1 and 1000 nM mitochondrial depolarizing agent CCCP (carbonyl cyanide 3-chlor-ophenylhydrazone). After incubation, cells were centrifuged, and

cell pellets were resuspended in 0.4 ml of DPBS and analyzed for JC-1 fluorescence by flow cytometry. The excitation/emission fluorescence for JC-1 is 514/529 nm (green) and 590 nm (red).

## Mitochondrial membrane potential assay (TMRE assay)

TMRE membrane potential kit from Abcam (Cambridge, MA) was used according to manufacturer's instructions. Control cells were seeded at a concentration of $1 \times 10^5$ cells per well while the PPID-6 and PPID-7 cells at a concentration of $1.7 \times 10^5$ cells per well in 6-well plates. After the initial 24 h incubation, the cultured media were replaced and cells incubated for additional 24 h to obtain the same 50–60% confluence. Then cells were exposed to two irradiations of 20 J/cm$^2$ UVA spaced 12 h apart for a total dose of 40 J/cm$^2$. 4 h after the second irradiation the TMRE was added to the media at 50 nM final concentration and cells were incubated for 20 min at 37 °C, 5% $CO_2$ (1000 nM FCCP was added to the positive control cells 10 min prior of TMRE). After incubation, cells were trypsinized, centrifuged, and cell pellets were resuspended in 0.4 ml of DPBS with 0.2% BSA and analyzed for TMRE fluorescence by flow cytometry. The excitation/emission fluorescence for TMRE is 549/575 nm.

## Mitochondrial permeability transition pore (MPTP) opening assay

MPTP opening was measured using the MitoProbe transition pore opening kit (Invitrogen, San Diego, CA). Control cells were seeded at a concentration of $1 \times 10^5$ cells per well while the PPID-6 and PPID-7 cells at a concentration of $1.7 \times 10^5$ cells per well in 6-well plates and incubated for 24 h. The second day, media were replaced and cells were incubated for additional 30 h in order to reach the same confluence of all cell lines (50–60%). Then the media were removed and replaced with warm Hank's balanced salt solution containing calcium (HBSS/Ca; Sigma-Aldrich, Saint Louis, MO) and cells were irradiated with a single dose of 20 J/cm2 UVA. 2 h after the irradiation, cells were trypsinized, collected and washed once with HBSS/Ca prior to performing the MPTP assay. Cells from each well were divided into three populations and placed into individual tubes. In parallel experiments, cells were loaded with calcein-AM alone or calcein-AM and $CoCl_2$ or calcein-AM, $CoCl_2$ and ionomycin and incubated for 15 min at 37 °C. Cells were centrifuged, washed, and cell pellets were resuspended in 0.4 ml of DPBS and analyzed for mitochondrial calcein fluorescence by flow cytometry analysis. The excitation/emission fluorescence for calcein-AM is 494/517 nm. Fluorescence intensity was calculated as a percentage by gating upon the positive and negative controls.

## Determination of mitochondrial superoxide

MitoSOX red mitochondrial superoxide indicator (Invitrogen, San Diego, CA) was used to detect superoxide, as a general measure of cellular oxidative stress in the mitochondria of live cells. Control cells were seeded at a concentration of $1 \times 10^5$ cells per well while the PPID-6 and PPID-7 cells at a concentration of $1.7 \times 10^5$ cells per well in 6-well plates. After 24 h, the media were replaced and cells incubated for additional 30 min. Immediately prior to irradiation, the media were removed and replaced with HBSS/Ca/Mg and cells were irradiated with a

single dose of 20 J/cm$^2$ UVA. Immediately after irradiation, HBSS/Ca/Mg was removed and HBSS/Ca/Mg containing 3 μM MitoSOX red was added to the cells. Cells were incubated at 37 °C for 30 min in dark, then washed with warm DPBS, trypsinized, centrifuged and resuspended in 0.4 ml of DPBS, and MitoSOX red fluorescence was analyzed by flow cytometry (excitation/emission fluorescence is 510/580 nm).

## Statistical analysis

Data were collected and analyzed to obtain the mean and SSD for three independent experiments. Statistical significance between any two groups was determined by the two-tailed Student's t-test, $P$ values less than 0.05 were considered to be significant.

## Results

### shRNA knock down CyP40 in HaCaT keratinocytes

We created two HaCaT keratinocyte cell lines with stably knocked-down cytosolic CyP40 gene. RT-PCR confirmed a 99% decrease of CyP40 expression in the PPID-6 cell line and a 90% decrease in the PPID-7 cell line compared to the control cell line transfected with empty vector (Fig. 1). There were no significant differences in expression levels of CyP40 between the control cell line transfected with empty vector and the parental untransfected HaCaT cells (data not shown). These two cell lines showed the same behavioral characteristics in all assays that were further performed.

### Lowered CyP40 gene expression levels reduce cellular proliferation

Cellular proliferation showed significantly lower growth of HaCaT cells with silenced CyP40 expression in comparison to the control
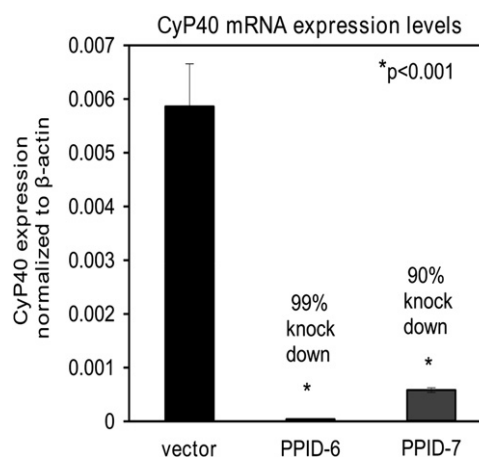


Fig. 1 – mRNA expression levels of CyP40 gene in control, PPID-6 and PPID-7 cell lines. Histogram is showing the levels of expression of CyP40 gene as analyzed by quantitative real-time PCR. Data represent means±SD of three independent samples for each cell line. At least three independent experiments were done. The asterisks indicate that PPID-6 and PPID-7 cells showed a statistically significant decrease in expression levels of CyP40 gene compared to control cells.

**Fig. 2 – Proliferation rate of PPID-6 and PPID-7 cells is significantly decreased in comparison with control cells. Cells were incubated in high glucose DMEM for 24, 48 and 72 h, respectively. Columns represent num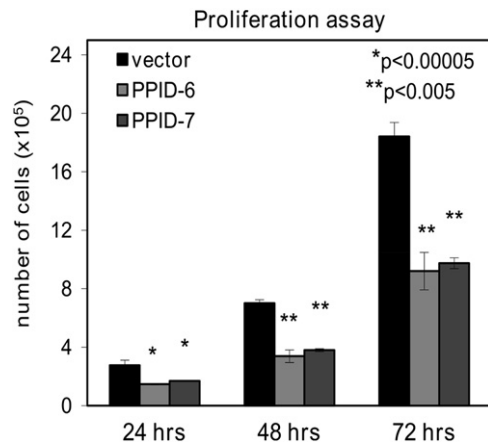bers of viable cells. Data represent means±SD of three independent samples for each cell line. At least three independent experiments were done. Asterisks indicate statistical differences compared to control cells.**

cells. After 24 h, there was a statistically significant difference in growth rate which was even more profound after 48 h. After 72 h, the number of living cells in control line was double in comparison to the PPID-6 and PPID-7 cell lines (Fig. 2), indicating a potential role of CyP40 as a regulator of cellular proliferation. Control cell lines that were transfected with empty vector had the same proliferation rate as untransfected parental HaCaT cells (data not shown). When the numbers of dead cells were counted, no differences between the cells transected with CyP40 and control cells transfected with empty vector were found, highlighting that the effect seen in CyP40 silenced cells was one of diminished cellular proliferation rather than enhanced death.

## CyP40 gene knocked down protects cell from death following UVA irradiation

To determine the effect of CyP40 expression knock down on keratinocyte cell death, we measured apoptosis for non-irradiated and for UVA-irradiated cells using both CyP40 knocked-down cell lines (PPID-6 and PPID-7) and control empty vector cell line. The conjugate of Annexin V, a protein with a high affinity for phosphatidylserine (PS), allows detection of cells undergoing early to late stages of apoptosis by flow cytometry analysis. PI was used to stain cells with altered membrane integrity which is typical for cells in the later stages of apoptosis or necrosis. Flow cytometry analysis revealed 90% viability in non-irradiated control cell samples and almost the same 85% viability in both PPID-6 and PPID-7 samples. However, after UVA irradiation the viability of control cells dropped down to 25% while the viability of PPID-6 and PPID-7 CyP40 silenced cells dropped down to 45% and 60%, respectively (Fig. 3A). These data demonstrate a significant protection of CyP40 knocked down cell lines against a UVA light in comparison to control cells resulting in higher survival rate. Furthermore, representative data from flow

cytometry (Fig. 3B) show that the process is mediated through apoptotic pathways rather than necrotic pathways.

## CyP40 knock down alters MMP and MPTP activity following UVA-irradiation

To analyze the effect of CyP40 expression knocked down on MPTP, we measured MMP and MPTP activity using flow cytometry. We used two fluorescent dyes, JC-1 and TMRE which are specific indicators of MMP, to evaluate if there are significant changes in the status of MMP between the PPI-6 and PPID-7 cells transfected with CyP40 and control cells exposed to UVA-irradiation. JC-1 accumulates in mitochondria where it forms aggregates in cells with high MMP and emits a red fluorescence. When MMP collapses there is a shift in JC-1 fluorescence from red to green. Non-irradiated control cells showed high MMP with red JC-1 staining and treatment with CCCP, a mitochondrial uncoupler, caused a complete shift from red to green fluorescence. Tetramethylrhodamine ethyl ester (TMRE) is a cell permeable, positively-charged, red-orange dye that readily accumulates in active mitochondria due to their relative negative charge. Depolarized or inactive mitochondria have decreased membrane potential and fail to sequester TMRE. FCCP (a mitochondrial uncoupler) depolarizes mitochondrial membrane completely and thus serves as a positive control. There was no significant difference in mitochondrial membrane potential status between all three non-irradiated cell lines. However, in UVA exposed cell lines, the measurements indicated that control cells show more sensitive response to UVA irradiation by manifesting low red/green ratio and low TMRE fluorescence. In PPID-6 and PPID-7 cell lines the red/green ratio and TMRE fluorescence is higher, indicating less sensitivity to UVA exposure (Fig. 4A–D). Our data showed that CyP40 knock down prevents MMP dissipation in keratinocytes.

To further evaluate MPTP opening in CyP40 knocked down cells, we monitored MPTP activity using calcein AM (cAM). Following UVA-irradiation, the cells were incubated with the acetoxymethyl (AM) ester of calcein which passively diffuses across the plasma membrane and accumulates in cytosolic compartments (including mitochondria). Once inside cells, intracellular esterases cleave the acetoxymethyl esters to liberate the very polar fluorescent dye calcein, which does not cross the mitochondrial or plasma membranes. In order to assess MPTP activity, we measured calcein fluorescence accumulated in the mitochondria by quenching cytosolic calcein with cobalt chloride $(CoCl_2)$. Flow cytometry analysis revealed that UVA-irradiated PPID-6 and PPID-7 cell lines had less loss of calcein fluorescence than it was observed in control cells (Fig. 5) indicating greater calcein AM retention in mitochondria (from a less active MPTP). Our data showed less active MPTP opening in CyP40 knocked down cell lines which are more resistant to UVA induced mitochondrial depolarization and MPTP opening in comparison to control cells.

## Mitochondrial superoxide induced by UVA exposure in CyP40-knocked down cell lines

In order to examine the ROS levels in CyP40 knocked down cell lines either exposed to UVA irradiation or not (UVA light is known as an intracellular ROS stimulator), we used a fluoroprobe for the specific detection of superoxide in the mitochondria of living cells. MitoSox red dye localizes specifically to the
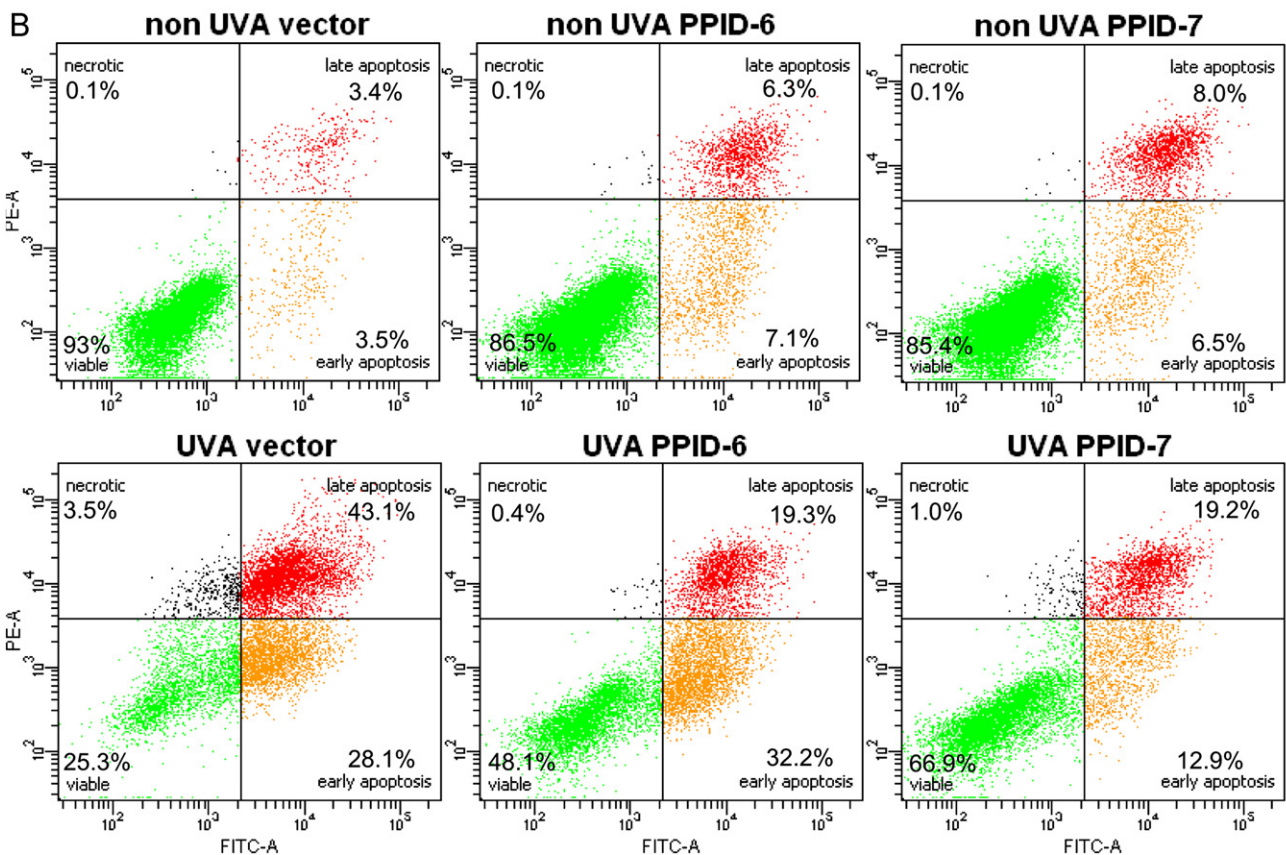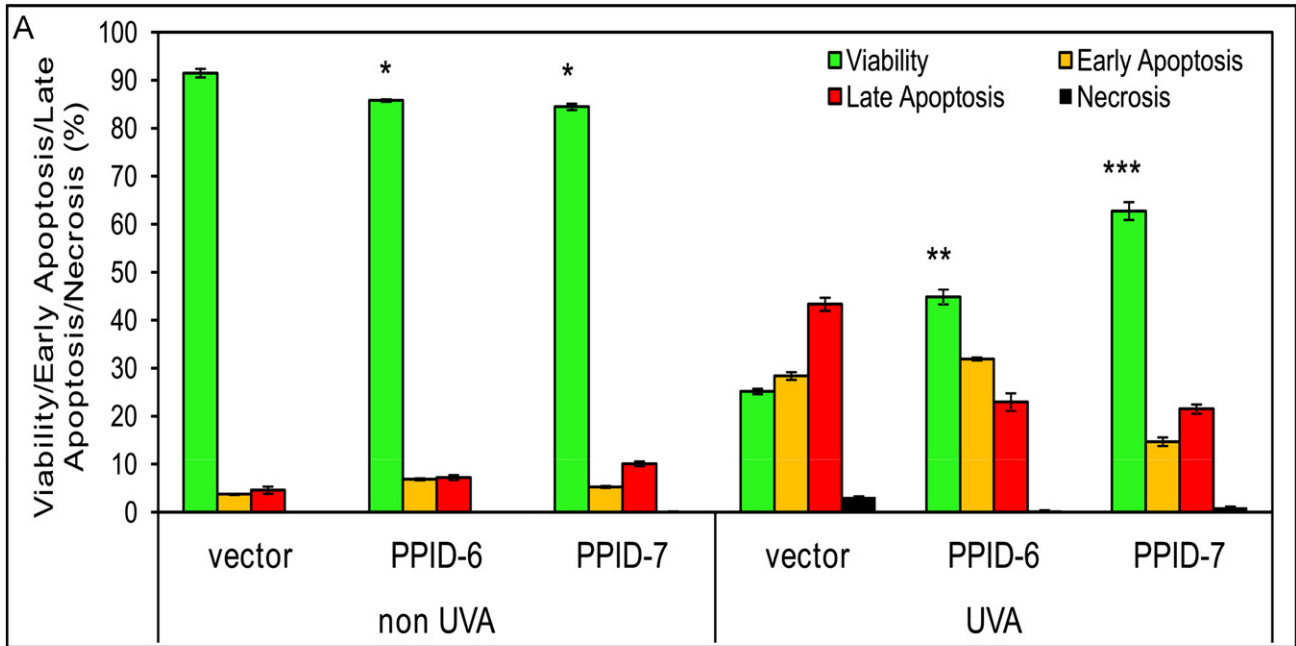
Fig. 3 – Cells with silenced CyP40 resist to UVA-induced apoptosis compared to control cells. (A) Bar graphs showing numbers of viable cells after the cells are either mock treated (0J UVA) or irradiated with 20J of UVA to induce apoptosis. Data represent means ± SD of three independent samples for each cell line. At least three independent experiments were done. Asterisks indicate significant differences compared to control cells and (B) Examples of representative data from flow cytometry.

mitochondria where it fluoresces after it is oxidized by super-oxide. Our results showed significantly lower levels of mitochon-drial superoxide after UVA irradiation in PPID-6 and PPID-7 cell lines than it was found in control cells. On the other hand, in non-irradiated samples there were observed slightly lower superoxide levels in PPID-6 and PPID-7 cells compared to control cells (Fig. 6A). Moreover, representative data from flow cytometry showed a significant difference in levels of superoxide between
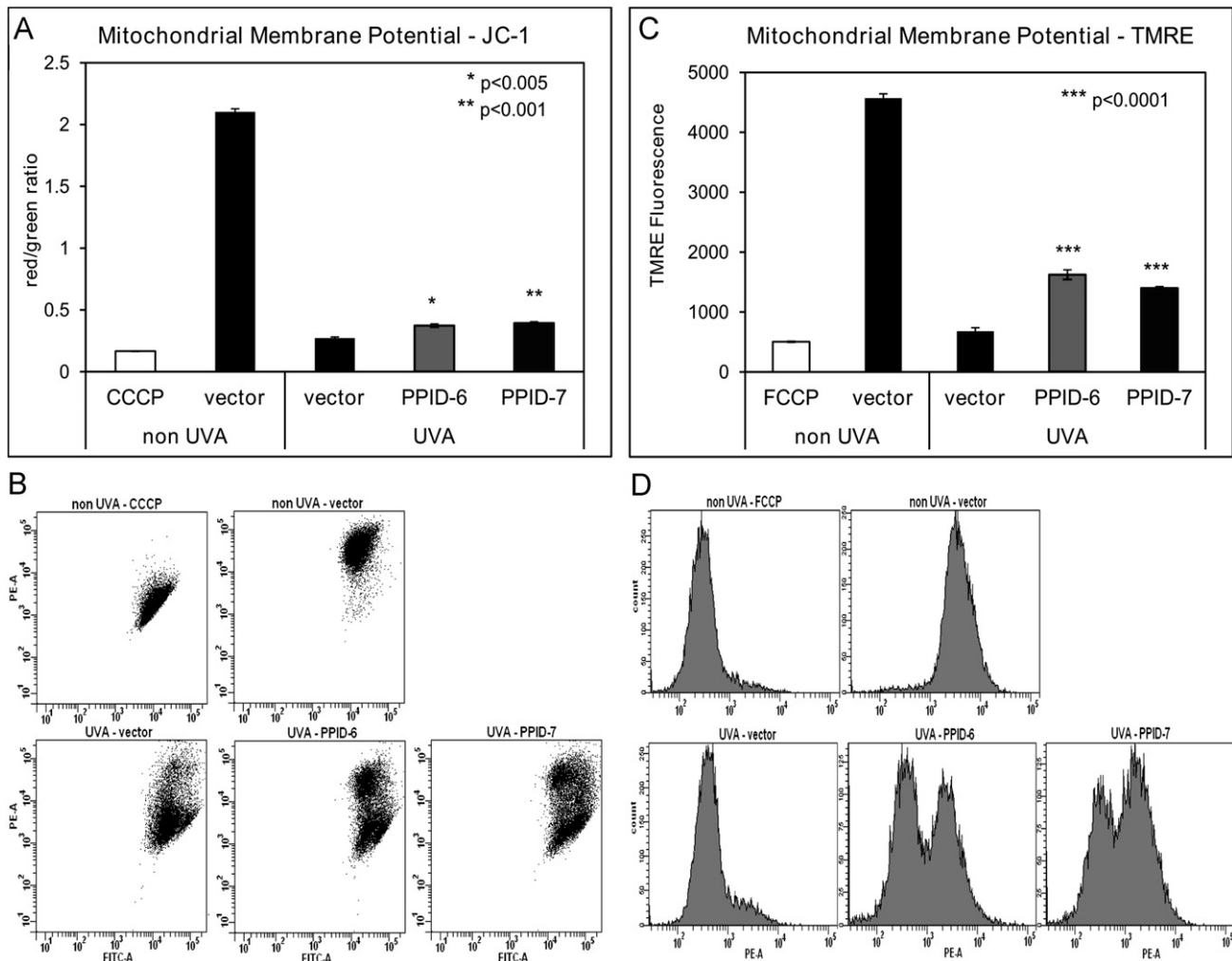
Fig. 4 – Mitochondrial membrane potential is lower in control cells compared to PPID-6 and PPID-7 after UVA irradiation. PPID-6, PPID-7 and control cells were twice irradiated with UVA (20 J/cm$^2$). (A) Mitochondrial depolarization was assessed as the fluorescence shift of JC-1 from red to green by flow cytometry analysis. (B) Examples of representative data from flow cytometry for JC-1 assay. (C) Mitochondrial depolarization was assessed as the TMRE fluorescence by flow cytometry analysis and (D) Examples of representative data from flow cytometry for TMRE assay. Data represent means $\pm$ SD of three independent samples for each cell line. At least three independent experiments were done. Asterisks above error bars indicate significant differences compared to control cells.

the cells that were exposed to UVA (higher in control cells than PPID-6 and PPID-7 cells; Fig. 6B).

## CyP40-knock down alters expression of mitochondrial pore proteins CyPD/PPIF, VDAC1, ANT2 and ANT3

Stable knock-down of cytosolic CyP40 expression was able to significantly affect the gene expression levels of other genes of mitochondrial pore including CyPD/PPIF, VDAC1, ANT2 and ANT3. Specifically, expression levels of VDAC1 were decreased by 52% in CyP40 silenced cells that were not exposed to UVA irradiation, the same effect observed in these cells after the UVA exposure. The expression levels of ANT2 and ANT3 were decreased in non UVA exposed CyP40 knocked down cells by 27% and 55%, respectively while there was seen significant decrease of 48% in ANT2 expression and 43% in ANT3 expression levels in these cells exposed to UVA irradiation. Moreover, there was observed 40% inhibition in

expression of mitochondrial 17 kDa CyPD/PPIF gene in cells with altered CyP40 levels that were either exposed to UVA or not. Generally, as it is shown in Supplemental Fig. 1, there is a significantly lower expression of mitochondrial pore genes in cells with CyP40 was stably knocked down compared to the control cells what indicates that altered CyP40 expression partially modulates expression of the most important genes involved in mitochondrial pore formation (MPTP).

## Discussion

In this study, we examined the consequences of altered expression of cytosolic 40 kDa CyP40 on mitochondrial functions of human keratinocytes. Our results showed an effect of CyP40 knock down on processes including the UVA-induced apoptosis, mitochondrial
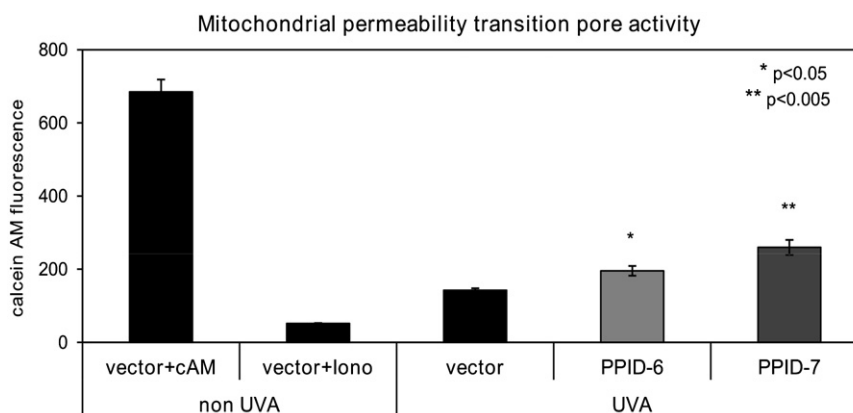
**Fig. 5 – Mitochondrial Permeability Transition Pore activity is higher in control cells than PPID-6 and PPID-7 cells after a single dose of UVA irradiation 20 J/cm². The MPTP was monitored by quantifying the fluorescence of calcein in the mitochondria of cells by flow cytometry. The cells were then loaded with calcein AM (cAM) and CoCl2 (cytosolic calcein quencher) to determine the calcein fluorescence in the mitochondria. Control cells were loaded with cAM alone cAM, CoCl2, and ionomycin (iono) which triggers pore opening and loss of mitochondrial calcein fluorescence. Data represent means±SD of three independent samples for each cell line. At least three independent experiments were done. Asterisks indicate significant differences compared to control cells.**

membrane potential, activity of mitochondrial pore along with the mRNA expression levels of its components, and ROS generation.

We generated two HaCaT keratinocyte cell lines with stable CyP40 knocked down by transfecting parental HaCaT cells with viral particles containing shRNA against CyP40 gene. We used two individual CyP40 shRNA constructs for stable transfection resulting in two cell lines named PPID-6 and PPID-7. As a control, parental cells were tranfected with an empty vector carrying only the antibiotic resistance to puromycin in order to ensure that viral particles themselves does not have any impact on behavior of parental HaCaT cells. RT-PCR confirmed 90%, respectively 99% knock down of CyP40 expression for both tested cell lines.

Cellular proliferation rate was examined and found to be quite altered in the cells with silenced CyP40 compared to control cells. A small but significant difference was observed after 24 h of incubation starting with the same number of cells for all three cell lines. This difference between control cells and cells with silenced CyP40 was even more significant after 48 h and 72 h. These results correspond with observation of Periyasamy et al. [27] who reported significantly slower growth of androgen-dependent prostate cancer cells after transient transfection using siRNA against cytosolic CyP40.

Cellular apoptosis was assessed by flow cytometry and revealed that the viability of PPID-6 and PPID-7 cells was always slightly lower than was in the control cells. Although the apoptosis was not increased profoundly in CyP40 silenced cells (only by 5%), this difference was statistically significant and always present. Our data indicate that CyP40 is an important component in the apoptotic processes since once it is stably knocked down in cells then the apoptotic rate is higher. On the other hand, this difference does not explain observed decrease in cellular growth of CyP40 knocked down cells; proliferation rate in CyP40 knocked down cells is about 50% lower compared to control cells while apoptosis is increased by only 5%. Hence, the compromised cell growth is not predominantly caused by increased apoptosis in these cells but is an effect of silenced CyP40 on cellular growth through affecting cell cycle.

Although the silencing of CyP40 in the cultured cells was found having a small pro-apoptotic effect, the effect was the opposite once the UVA light was added to the system. Under standard laboratory conditions (without UVA exposure), PPID-6 and PPID-7 cells had slightly lower survival rates compared to control cells. Importantly, the UVA irradiation caused the opposite effect, showing that control cells responded with significantly higher apoptotic rate compared to the cells with CyP40 knocked down expression. Although UVA also triggered apoptosis in PPID-6 and PPID-7 cell lines, the response to UVA irradiation was notably diminished since the number of viable cells was significantly higher than in control cells and apoptosis was not observed close to the level of control cells. These findings are similar to those of Favreau et al. [28] who studied the effect of CyP40 silencing in human neuronal cell lines. Specifically, using the same viral constructs as used in our study they were able to protect CyP40 knock down cells against apoptosis after exposing the neural cells to human coronavirus. Although they incorrectly identified the 40 kDa CyP40 as the 17 kDa mitochondrial CyPD, the overall data did show that CyP40 silencing resulted in significant protection from cell death after inducing apoptosis by viral mechanism.

We also tested the response of MMP as well as MPTP opening in response to UVA exposure. Both experiments revealed that mitochondrial response to UVA irradiation is lower in CyP40 knocked cells than in control cells by showing significantly more stable MMP and less active MPTP what correlates with lower apoptosis in these cells. We also examined the ROS levels with and without UVA irradiation stimuli by focusing on mitochondrial superoxide. PPID-6 and PPID-7 cell lines were found to have significantly lower amount of superoxide after UVA irradiation but slightly higher level without UVA stimuli what correlates with the results obtained from the apoptotic assays. Furthermore, we conducted a mechanistic study focused on mitochondrial pore genes. It was already suggested in literature that suppression of mitochondrial pore proteins could be one of the possible cancer therapy treatments (VDAC [29,30], ANTs [31,32] and CyPD [33]). Here, we have demonstrated that silencing of
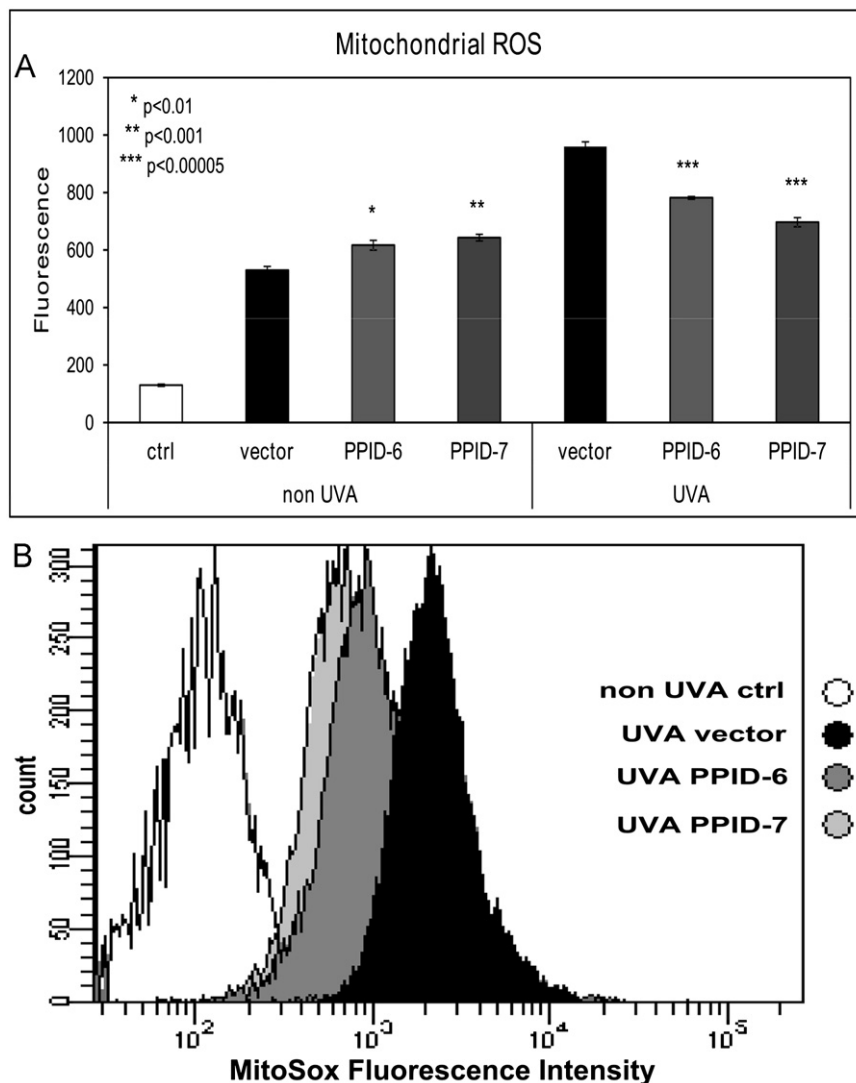
**Fig. 6 – Oxidative stress is significantly elevated in UVA-irradiated (20 J/cm$^2$) control cells compared to UVA-irradiated PPID-6 and PPID-7 cells and slightly less elevated without UVA irradiation. (A) Data represent the amount of mitochondrial superoxide as measured by the linear mean of MitoSox Red fluorescence by flow cytometry analysis (MitoSox Red dye was added to all samples excluding negative control sample, labeled as ctrl). Data represent means ± SD of three independent samples for each cell line. At least three independent experiments were done. Asterisks above error bars indicate significant differences compared to control cells and (B) Examples of representative data for UVA irradiated cells from flow cytometry.**

cytosolic CyP40 is partially altering (down-regulating) the expression of genes coding the most important mitochondrial pore proteins including VDAC1, ANT2, ANT3 and CyPD/PPIF.

In addition to our studies, Siu et al. [34] transiently knocked down cytosolic CyP40 using siRNA sequence for 40 kDa CyP40 (although incorrectly reported as the mitochondrial 17 kDa CyPD) and have observed that silencing of cytosolic CyP40 eliminated function of mitochondria by inhibiting MPTP as well as we proved in our study. Moreover, they pointed out the interactions between CyP40 and Bax protein as one of the major components promoting mitochondrial apoptosis. In addition to the Bax interaction, Favreau et al. [28] showed that inhibition of cytosolic CyP40 alters release of apoptosis-inducing factor (AIF) and cytochrome c from mitochondria. Bax protein seems to be one of the major partners of CyP40 since its translocation toward mitochondria after an induced stress of either chemical, physical or biological origin leads to series

of mitochondrial responses such as accumulation of ROS, increasing Ca$^{2+}$ levels, and formation of pores in the mitochondrial membrane which allows for the release of pro-apoptotic factors such as cytochrome c and AIF [35]. Generally, these studies as well as our observations indicate that it is not solely mitochondrial 17 kDa CyPD that is regulating apoptosis at the mitochondrial level, but also the cytosolic CyP40 appears to be a factor which can partially regulate important mitochondrial functions including pore formation.

In conclusion, in our study we show for the first time that silencing of cytosolic 40 kDa CyP40 causes a protective effect against UVA-induced apoptosis in human keratinocytes and this is most likely produced through an alteration of mitochondrial function and specifically mitochondrial ROS. Thus, our data show that diminished levels of CyP40 expression are associated with increased resistance to UVA-induced apoptosis. A more intensive

investigation focused on cytosolic CyP40 interactions with other mitochondrial proteins and other pro-apoptotic components like Bax protein and contrarily anti-apoptotic agents like antioxidants is in order to elucidate if these pathways may be involved in the enhanced tumorigenesis seen in the skin of organ transplant recipients who take CsA to prevent grafted organ rejection.

Medications such as CsA that inhibit the activity of CyP40, or other therapies that have the result of lowering CyP40 levels may have an undesirable effect in the skin of promoting tumors or by generating populations of cells that are resistant to therapeutic strategies such as photodynamic therapy or photochemo-therapy that are designed to induce apoptosis in tumor cells. As a corollary, therapeutic strategies to increase CyP40 levels in cutaneous malignancies may allow for UVA to be used as a paired therapeutic modality to treat skin cancers with depths that are penetrable by irradiation with UVA. Anti-rejection drugs that maintain sensitivity of keratinocytes to UV-induced apoptosis without binding of the CyP40 immunophilin may also help reduce the burden and severity of skin cancers faced in the organ transplant recipient population.

## Conflict of interest

The authors declare no conflict of interest.

## Acknowledgments

## Appendix A. Supporting information

Supplementary data associated with this article can be found in the online version at http://dx.doi.org/10.1016/j.yexcr.2012.11.016.

## REFERENCES

[1] L. Andreeva, R. Heads, C.J. Green, Cyclophilins and their possible role in the stress response, Int. J. Exp. Pathol. 80 (1999) 305–315.

[2] V. Giorgio, M.E. Soriano, E. Basso, E. Bisetto, G. Lippe, M.A. Forte, P. Bernardi, Cyclophilin D in mitochondrial pathophysiology, BBA-Bioenergetics 2010 (1797) 1113–1118.

[3] P. Bernardi, A. Rasola, The mitochondrial permeability transition pore and its involvement in cell death and in disease pathogenesis, Apoptosis 12 (2007) 815–833.

[4] A.P. Halestrap, What is the mitochondrial permeability transition pore?, J. Mol. Cell Cardiol. 46 (2009) 821–831.

[5] Y. Suzuki, T. Yoshimaru, T. Inoue, C. Ra, Mitochondrial $Ca^{2+}$ flux is a critical determinant of the $Ca^{2+}$ dependence of mast cell degranulation, J. Leukocyte Biol. 79 (2006) 508–518.

[6] L.J. Kieffer, T. Thalhammer, R.E. Handschumacher, Isolation and characterization of a 40-kDa cyclophilin-related protein, J. Biol. Chem. 267 (1992) 5503–5507.

[7] W.B. Pratt, M.D. Galigniana, J.M. Harrell, D.B. DeFranco, Role of hsp90 and the hsp90-binding immunophilins in signalling protein movement, Cell Signal 16 (2004) 857–872.

[8] T. Ratajczak, B.K. Ward, R.F. Minchin, Immunophilin chaperones in steroid receptor signalling, Curr. Top Med. Chem. 3 (2003) 1348–1357.

[9] P.D. Reynolds, Y. Ruan, D.F. Smith, J.G. Scammell, Glucocorticoid resistance in the squirrel monkey is associated with overexpression of the immunophilin FKBP51, J. Clin. Endocr Metab. 84 (1999) 663–669.

[10] A. Carrello, R.K. Allan, S.L. Morgan, B.A. Owen, D. Mok, B.K. Ward, R.F. Minchin, D.O. Toft, T. Ratajczak, Interaction of the Hsp90 cochaperone cyclophilin 40 with Hsc70, Cell Stress Chaperones 9 (2004) 167–181.

[11] S.C. Nair, R.A. Rimerman, E.J. Toran, S. Chen, V. Prapapanich, R.N. Butts, D.F. Smith, Molecular cloning of human FKBP51 and comparisons of immunophilin interactions with Hsp90 and progesterone receptor, Mol. Cell Biol. 17 (1997) 594–603.

[12] C. Radanyi, B. Chambraud, E.E. Baulieu, The ability of the immunophilin FKBP59-HBI to interact with the 90-kDa heat shock protein is encoded by its tetratricopeptide repeat domain, Proc. Nat. Acad. Sci. USA 91 (1994) 11197–11201.

[13] S. Periyasamy, M. Warrier, M.P.M. Tillekeratne, W.N. Shou, E.R. Sanchez, The immunophilin Ligands cyclosporin a and FK506 suppress prostate cancer cell growth by androgen receptor-dependent and -independent mechanisms, Endocrinology 148 (2007) 4716–4726.

[14] B.K. Ward, P.J. Mark, D.M. Ingram, R.F. Minchin, T. Ratajczak, Expression of the estrogen receptor-associated immunophilins, cyclophilin 40 and FKBP52, in breast cancer, Breast Cancer Res. Treat. 58 (1999) 267–280.

[15] P.J. Mark, B.K. Ward, P. Kumar, H. Lahooti, R.F. Minchin, T. Ratajczak, Human cyclophilin 40 is a heat shock protein that exhibits altered intracellular localization following heat shock, Cell Stress Chaperones 6 (2001) 59–70.

[16] B.K. Ward, P. Kumar, G.R. Turbett, J.E. Edmondston, J.M. Papadimitriou, N.G. Laing, D.M. Ingram, R.F. Minchin, T. Ratajczak, Allelic loss of cyclophilin 40, an estrogen receptor-associated immunophilin, in breast carcinomas, J. Cancer Res. Clin. Oncol. 127 (2001) 109–115.

[17] A. Galat, Peptidylprolyl cis/trans isomerases (immunophilins): biological diversity–targets–functions, Curr. Top. Med. Chem. 3 (2003) 1315–1347.

[18] A. Nicolli, E. Basso, V. Petronilli, R.M. Wenger, P. Bernardi, Interactions of cyclophilin with the mitochondrial inner membrane and regulation of the permeability transition pore, and cyclosporin A-sensitive channel, J. Biol. Chem. 271 (1996) 2185–2192.

[19] K.G. Norman, J.A. Canter, M.J. Shi, G.L. Milne, J.D. Morrow, J.E. Sligh, Cyclosporine A suppresses keratinocyte cell death through MPTP inhibition in a model for skin cancer in organ transplant recipients, Mitochondrion (2010) 94–101.

[20] D.B. Zorov, M. Juhaszova, Y. Yaniv, H.B. Nuss, S. Wang, S.J. Sollott, Regulation and pharmacology of the mitochondrial permeability transition pore, Cardiovasc. Res. 83 (2009) 213–225.

[21] K. Hoffmann, L.T. Kakalis, K.S. Anderson, I.M. Armitage, R.E. Handschumacher, Expression of human cyclophilin-40 and the effect of the His141—>Trp mutation on catalysis and cyclosporin A binding, Eur. J. Biochem. 229 (1995) 188–193.

[22] X.S. Zhang, B.S. Rosenstein, Y. Wang, M. Lebwohl, H.C. Wei, Identification of possible reactive oxygen species involved in ultraviolet radiation-induced oxidative DNA damage, Free Radical Bio. Med. 23 (1997) 980–985.

[23] M.A. Bachelor, G.T. Bowden, Ultraviolet A-induced modulation of Bcl-XL by p38 MAPK in human keratinocytes: post-transcriptional regulation through the 3'-untranslated region, J. Biol Chem. 279 (2004) 42658–42668.

[24] P.K. Waster, K.M. Ollinger, Redox-dependent translocation of p53 to mitochondria or nucleus in human melanocytes after UVA- and UVB-induced apoptosis, J. Invest Dermatol. 129 (2009) 1769–1781.

[25] J.Z. Boyer, J. Jandova, J. Janda, F.R. Vleugels, D.A. Elliott, J.E. Sligh, U.V.A. Resveratrol-sensitized, induced apoptosis in human

keratinocytes through mitochondrial oxidative stress and pore opening, J. Photochem. Photobiol. B 113 (2012) 42–50.

[26] A. Valencia, I.E. Kochevar, Ultraviolet A induces apoptosis via reactive oxygen species in a model for Smith–Lemli–Opitz syndrome, Free Radical Biol. Med. 40 (2006) 641–650.

[27] S. Periyasamy, T. Hinds Jr., L. Shemshedini, W. Shou, E.R. Sanchez, FKBP51 and Cyp40 are positive regulators of androgen-dependent prostate cancer cell growth and the targets of FK506 and cyclosporin A, Oncogene 29 (2010) 1691–1701.

[28] D.J. Favreau, M. Meessen-Pinard, M. Desforges, P.J. Talbot, Human coronavirus-induced neuronal programmed cell death is cyclophilin d dependent and potentially caspase dispensable, J. Virol. 86 (2012) 81–93.

[29] I. Koren, Z. Raviv, V. Shoshan-Barmatz, Downregulation of voltage-dependent anion channel-1 expression by RNA interference prevents cancer cell growth in vivo, Cancer Biol. Ther. 9 (2010) 1046–1052.

[30] E. Simamura, H. Shimada, T. Hatta, K. Hirai, Mitochondrial voltage-dependent anion channels (VDACs) as novel pharmacological targets for anti-cancer agents, J. Bioenerg. Biomembr. 40 (2008) 213–217.

[31] A. Chevrollier, D. Loiseau, P. Reynier, G. Stepien, Adenine nucleotide translocase 2 is a key mitochondrial protein in cancer metabolism, Biochim. Biophys. Acta 1807 (2011) 562-567.

[32] J.Y. Jang, Y.K. Jeon, Y. Choi, C.W. Kim, Short-hairpin RNA-induced suppression of adenine nucleotide translocase-2 in breast cancer cells restores their susceptibility to TRAIL-induced apoptosis by activating JNK and modulating TRAIL receptor expression, Mol. Cancer 9 (2010) 262.

[33] G. Chen, J. Izzo, Y. Demizu, F. Wang, S. Guha, X. Wu, M.C. Hung, J.A. Ajani, P. Huang, Different redox states in malignant and nonmalignant esophageal epithelial cells and differential cytotoxic responses to bile acid and honokiol, Antioxid. Redox Signal 11 (2009) 1083–1095.

[34] W.P. Siu, P.B. Pun, C. Latchoumycandane, U.A. Boelsterli, Bax-mediated mitochondrial outer membrane permeabilization (MOMP), distinct from the mitochondrial permeability transition, is a key mechanism in diclofenac-induced hepatocyte injury: multiple protective roles of cyclosporin A, Toxicol. Appl. Pharmacol. 227 (2008) 451–461.

[35] R. Kumarswamy, S. Chandna, Putative partners in Bax mediated cytochrome-c release: ANT, CypD, VDAC or none of them?, Mitochondrion 9 (2009) 1–8.